Available online at www.sciencedirect.com
SCIENCE DIRECT®
ELSEVIER
International Journal of Solids and Structures 43 (2006) 4136–4153
INTERNATIONAL JOURNAL OF SOLIDS and STRUCTURES
www.elsevier.com/locate/ijsolstr

Influence of penetration depth and mechanical properties on contact radius determination for spherical indentation

X. Hernot *, O. Bartier, Y. Bekouche, R. El Abdi, G. Mauvoisin

LARMAUR, FRE-CNRS 2717, Bât 10B, Université de Rennes 1, Campus de Beaulieu, 35042 Rennes Cedex, France

Received 27 May 2005
Available online 20 July 2005

Abstract

Knowledge of the relationship between the penetration depth and the contact radius is required in order to determine the mechanical properties of a material starting from an instrumented indentation test. The aim of this work is to propose a new penetration depth–contact radius relationship valid for most metals which are deformed plastically by parabolic and spherical indenters. Numerical simulation results of the indentation of an elastic–plastic half-space by a frictionless rigid paraboloïd of revolution show that the contact radius–indentation depth relationship can be represented by a power law, which depends on the reduced Young's modulus of the contact, on the strain hardening exponent and on the yield stress of the indented material. In order to use the proposed formulation for experimental spherical indentations, adaptation of the model is performed in the case of a rigid spherical indenter. Compared to the previous formulations, the model proposed in the present study for spherical indentation has the advantage of being accurate in the plastic regime for a large range of contact radii and for materials of well-developed yield stress. Lastly, a simple criterion, depending on the material mechanical properties, is proposed in order to know when piling-up appears for the spherical indentation.

Keywords: Spherical; Indentation; Contact radius; Elastic–plastic solids

1. Introduction

Instrumented indentation experiments, where load and depth of penetration are measured continuously, enable an evaluation of mechanical properties such as Young's modulus, work hardening exponent and

* Corresponding author. Tel.: +33 2 2323 6148; fax: +33 2 2323 6111.
E-mail address: xavier.hernot@univ-rennes1.fr (X. Hernot).

0020-7683/$ - see front matter © 2005 Elsevier Ltd. All rights reserved.
doi:10.1016/j.ijsolstr.2005.06.007

yield stress (Oliver and Pharr, 1992; Taljat et al., 1998; Kucharski and Mröz, 2001; Beghini et al., 2000; Sundararajan and Tirupataiah, 1994). This assessment requires precise knowledge of the true contact area between the indenter and the indented material, which depends on the way the material is deformed at the contact boundary. During an indentation test, the material around the contact area can be deformed upwards or downwards along the z axis where load is applied. This behavior, called piling up in the first case and sinking-in in the second case, is affected by the mechanical properties of the indented materials. Indeed, such surface deformation modes influence hardness measurements as the true contact area between the indenter and the specimen increases in the case where piling-up predominates, and decreases in the event that sinking-in predominates (Bolshakov and Pharr, 1998). On the other hand, if the development of piling-up and sinking-in is not taken into account, errors of up to 20% can be obtained for the Young's modulus value (Bolshakov and Pharr, 1998; Eskner and Sandström, 2004).

Many studies have been realized in order to determine a relationship between the contact area and the indenter displacement measured during the continuous indentation test.

Numerical and experimental work on spherical indentation tests provided the following general formulation (Hill et al., 1989; Taljat et al., 1998; Alcala et al., 2000; Kucharski and Mröz, 2001):

$$a^2 = 2c^2hR \tag{1}$$

where a is the contact radius, h is the maximum penetration depth underneath the original surface and R is the indenter radius (Fig. 1).

In this equation, c^2 quantifies the degree of piling-up and sinking-in during the indentation test; $c^2 > 1$ indicates piling-up, whereas, $c^2 < 1$ accounts for sinking-in.

In the case of material which is elastically deformed by indentation, c^2 is constant and equal to 0.5 (Sneddon, 1965). When the stress under the indenter is higher than the yield stress of the indented material, this parameter increases with the indent depth during a stage called "elastic–plastic indentation regime" (Mesarovic and Fleck, 1999). For higher indent depths, the c^2 parameter is again found constant during a stage called "fully plastic regime" (Mesarovic and Fleck, 1999).

For this last indentation regime, c^2 is often linked to the strain hardening exponent of the indented material (Matthews, 1980; Hill et al., 1989; Taljat et al., 1998; Alcala et al., 2000; Kucharski and Mröz, 2001). It is generally recognized that piling-up predominates when the hardening exponent is weak. However, results of finite element simulations of spherical indentation showed that the yield stress of the indented material has an influence on the c^2 parameter (Beghini et al., 2000). For a given strain hardening exponent and Young's modulus, the smaller the yield stress, the more the pile up predominates. Moreover, Mesarovic and Fleck (1999) observed that, compared with the frictionless case, sticking friction reduces the amount of pile-up at the edge of the indenter and leads to consistently smaller contact area for a given depth. More recently, it was also shown that an increase in friction coefficient between a spherical indenter and the

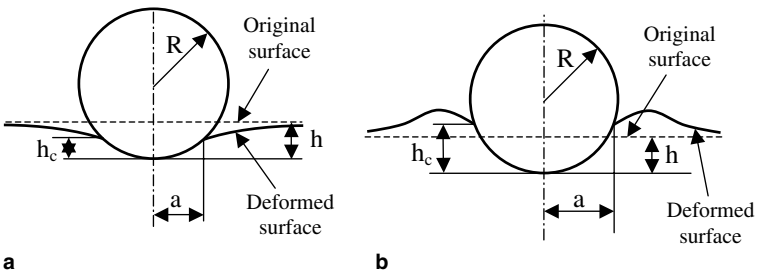

Fig. 1. Schematic representation of sinking-in (a) and piling-up (b) of material around spherical indents and sharp indents.

indented material can reduce the contact radius when considerable piling-up occurs (Taljat and Pharr, 2004).

To our knowledge, no relationship between the contact area and the indenter displacement has been proposed when the indentation regime is ''elastic–plastic''. Moreover, the indentation stage called ''Fully-plastic regime'', in which the proposed formulation for c^2 is considered as valid, is not clearly defined.

It is assumed that the fully plastic regime is reached when the plastic deformation, which occurs in the material beneath the indenter, reaches the free material surface and when the following equation is valid (Tabor, 1951; Johnson, 1985):

$$\frac{P_m}{\sigma_R} = \psi \tag{2}$$

where P_m is the average indentation pressure, σ_R is the stress corresponding to the indentation representative plastic strain ($\epsilon_R = 0.2a/R$, in the case of spherical indentation (Tabor, 1951)) and ψ is a constant, called ''constrain factor'', essentially dependent on the material mechanical properties (Taljat et al., 1998; Sundararajan and Tirupataiah, 1994). In the case of spherical indentation, the transition between the ''elastic–plastic'' and the ''fully plastic'' stages, in term of a/R value, depends on the E^*/σ_R or E^*/σ_y ratio, where E^* is the reduced elastic modulus of the contact and σ_y is the yield stress of the indented material (Mesarovic and Fleck, 1999; Johnson, 1985; Park and Pharr, 2004). On the basis of results of different experimental and numerical indentation tests by spheres, Johnson (1985) showed that fully plastic deformation is reached at a value $E^*a/(\sigma_y R) \approx 40$. For elastic-ideally plastic solids, ψ increases until the ratio $E^*a/(\sigma_y R)$ is equal to 40–50 (Mesarovic and Fleck, 1999). More recently, for a range of E^*/σ_y ratio, which includes most metals, Park and Pharr (2004) showed that full plasticity is achieved when the value of the ratio $E^*a/(\sigma_y R)$ is about equal to 66.

For spherical indentation, Mesarovic and Fleck (1999) define a new regime called ''plastic similarity regime'' inside the ''fully plastic regime'', in which Eqs. (1) and (2) are both valid. By observing the results of Mesarovic and Fleck (1999), a difference can be noted between the lower limit of the ''fully plastic regime '' determined by Eq. (2) and the lower limit of the ''plastic similarity regime'' determined by Eqs. (1) and (2). For example, in the case of E^*/σ_y ratio equal to 10,000, ψ is constant when $E^*a/(\sigma_y R)$ is about equal to 40–50 and c^2 is constant when $E^*a/(\sigma_y R)$ reaches the value of 1000. For smaller E^*/σ_y ratios, Mesarovic and Fleck (1999) show that the plastic similarity regime is never reached since c^2 increases in the elastic–plastic regime and immediately falls with increasing contact size in a stage called ''finite deformation regime''. For the authors, the drop in c^2 value for large contact sizes represents the failure of the assumptions involved in the similarity solution, especially the assumption of infinitesimal strain kinematics and the boundary conditions of uniform normal velocity. As the contact size increases, the tangential velocity of points in contact with the indenter deviates from the horizontal, so that the uniform vertical velocity condition ceases to be appropriate. We can notice that the similarity solution was also determined with the assumption that geometric profile of the indenter can be represented by a power-law relationship. This assumption includes indentation by a rigid sphere, since, for small contact sizes, the profile of a sphere can be approximated by a paraboloïd of revolution. For large contact sizes, the failure of this assumption in the case of spherical indentation can also explain the drop in the $a^2/2hR$ ratio.

To summarize, when plasticity occurs, the contact radius–penetration depth relation (1) gives a constant c^2 only in a stage called ''similarity regime'', the range of which depends on the ratio $E^* a/(\sigma_y R)$ or is never valid if the E^*/σ_y ratio is smaller than 1000, which is the case of most materials used in industry (Mesarovic and Fleck, 1999).

The aim of this work is to propose a new relationship between the penetration depth of a spherical indenter, h, and the contact radius, a, valid for most usual metals, in elastic–plastic and fully plastic regimes. Firstly, after analysing the different c^2 formulations proposed in the literature, results of numerical

simulations of the indentation of an elastic–plastic half-space by a frictionless rigid paraboloïd of revolution are presented. This type of indenter is used in order to obtain a simple relationship between a and h when plasticity occurs and to avoid the problem of geometrical singularity which arises in spherical indentation for high contact radius values. Indeed, when the penetration depth become close to R value, the derivative of the function $a(h)$ tends toward to 0 in the case of spherical indentation, i.e the curve $a(h)$ has a horizontal asymptote. This result is not coherent with that obtained by the Eq. (1) (the derivative of the function $a(h)$ is equal to c^2 for depth equal to R). Because the curve $a(h)$ does not have a horizontal asymptote for parabolic indentation, the h–a relationship will be valid for contact radius values higher than R. Starting from the finite element results, a new model of the a–h relationship, valid in the plastic regime is proposed for the parabolic indentation. Then, in order to use the proposed formulation for experimental spherical indentations, adaptation of the model is performed in the case of a rigid spherical indenter. On the basis of numerical simulations and theoretical results, the validity of the c^2 formulations proposed to describe the a–h relationship in the fully plastic regime is discussed. Finally, a simple criterion, depending on the material mechanical properties, is proposed in order to know when piling-up appears for the spherical indentation.

2. Overview of the theory

Norbury and Samuel (1928) were among the first to show that the profile of the surface indended by a sphere is characterized by piling-up or sinking-in depending on the hardening properties of the material. The level of contact perimeters, experimentally determined by these authors after unloading, shows that annealed metals, which are fully capable of hardening, exhibit sinking-in. On the contrary, cold-worked metals showing almost perfectly plastic behavior are characterized by piling-up.

Moreover, they notice a relationship between the ratio of $(h_c - h)/h$ and $(n + 2)$, where h_c is the contact depth (Fig. 1) and $(n + 2)$ the exponent of the Meyer law (Meyer, 1908) given by

$$F = ka^{n+2} \tag{3}$$

in which, F is the applied load and k and n are material constants. Further work by O-Neill (1944) and Tabor (1951), showed that, for a wide range of materials, the n value was equal to the strain hardening exponent of the following tensile behavior law:

$$\sigma = K\varepsilon^n \tag{4}$$

where σ is the uniaxial true stress, K is the strength coefficient, ε is the true plastic strain and n is the strain hardening exponent.

According to this rule, Matthews (1980) proposed the following equation as a fit to the Norbury and Samuel h_c/h versus n data obtained after loading, at a depth for which a/R was mostly between 0.4 and 0.8, and unloading:

$$\frac{h_c}{h} = \frac{1}{2}\left(1 + \frac{n}{2}\right)^{2\left(\frac{1-n}{n}\right)} \tag{5}$$

If the shape of the sphere can be approximated by a parabolic curve or for small displacements of the spherical indenter ($h_c \ll R$), Eq. (5) can be expressed by using the c^2 parameter (see Eq. (1)) introduced by Hill et al. (1989) as follows:

$$c^2 = \frac{a^2}{2hR} = \frac{1}{2}\left(1 + \frac{n}{2}\right)^{2\left(\frac{1-n}{n}\right)} \tag{6}$$

By using these equations, we can observe that, piling-up occurs, i.e h_c/h and c^2 are higher than 1, when n is smaller than approximately 0.25.

More recently, Hill et al. (1989) conducted a theoretical and numerical study of the spherical indentation test using a nonlinear elastic constitutive model for the indented material. According to the authors, this model, equivalent to a rigid/plastic behavior law for a Brinell test, should be applicable for elastic–plastic material, as metals, over most of the plastic domain once the Meyer regime is established. The results of the theoretical study of the spherical indentation test, show that the speculative formulae of Matthews (1980) is incompatible with the pressure distribution. From the results of this theoretical study and FE computations, Hill et al. (1989) proposed a new relationship for c^2 depending on n valid for the loaded state, namely:

$$c^2 = \frac{5}{2}\left(\frac{2-n}{4+n}\right) \tag{7}$$

It is important to notice that in this equation, the invariant c^2 only depends on n and cannot be influenced by the yield stress σ_y and the Young's modulus E of the indented material and the friction coefficient α between the indenter and the indented material because of the model used by the authors.

Another formulation of c^2, valid for materials of elastic–plastic constitutive behavior, was proposed by Taljat et al. (1998) using the results of finite element simulations. For numerical simulations, the plastic constitutive behavior was taken to follow J_2-associated flow theory with rate-independent deformation and isotropic hardening. The plastic strain-hardening was represented by a power curve similar to that given in Eq. (4) and Von Mises yield criterion was assumed. The c^2 formulation, determined using computed FE data obtained for an $\sigma_y/E = 1/500$ material, a friction coefficient equal to 0.2 and a a/R ratio equal to 0.5, (Taljat et al., 1998) is

$$c^2 = \frac{1}{4}\left(5 - 3n^{0.7}\right) \tag{8}$$

As for the formulation proposed by Hill et al. (1989), the invariant c^2 of Eq. (8) cannot be influenced by σ_y, E and α because of the assumptions of the model used by Taljat et al. (1998).

The Norbury and Samuel data (1928) were also used by Alcala et al. (2000) in order to propose another c^2 formulation. These data and experimental results, obtained for metals with σ_y/E ranging between 1/272 and 1/114, led to the following equation:

$$c^2 = 1.276 - 1.748n + 2.451n^2 - 1.469n^3 \tag{9}$$

We can notice that as for the other formulations, c^2 depends only on n in this last equation. However, it should be specified that Eq. (9) is obtained by fitting experimental data. Consequently, this equation does not perfectly represent the evolution of c^2 according to n. Moreover, the small range of σ_y/E values of the metals tested by Alcala et al., does not allow to show if E or σ_y has an influence on c^2.

Furthermore, the influence of E or σ_y on c^2 was shown by Beghini et al. (2000) thanks to finite element simulations of the spherical indentation of elastic–plastic materials for which the σ_y/E ratio is in the range of 1/1050 to 1/262. The results show that the higher the value of σ_y/E ratio, the larger the sinking-in that is developed. The same behaviour was found for conical indentation by Mata and Alcala (2004) for materials with σ_y/E ratio between 1/4000 and 1/70.

In conclusion, the strain hardening exponent strongly affects the surface deformation around the contact area. Fig. 2 shows that the different formulations give similar results. In Fig. 2, it can be seen that the different formulations predict that piling-up and sinking-in occur for values of n which are respectively smaller and larger than 0.25. However, the yield stress and the Young's modulus have a considerable influence on the piling-up and sinking development (Beghini et al. (2000); Mata and Alcala (2004). The influence of these parameters on the c^2 parameter value was not taken into account in the formulations because of the calculus assumptions or because of the behavior law of the indented material (Hill et al., 1989; Taljat et al., 1998).

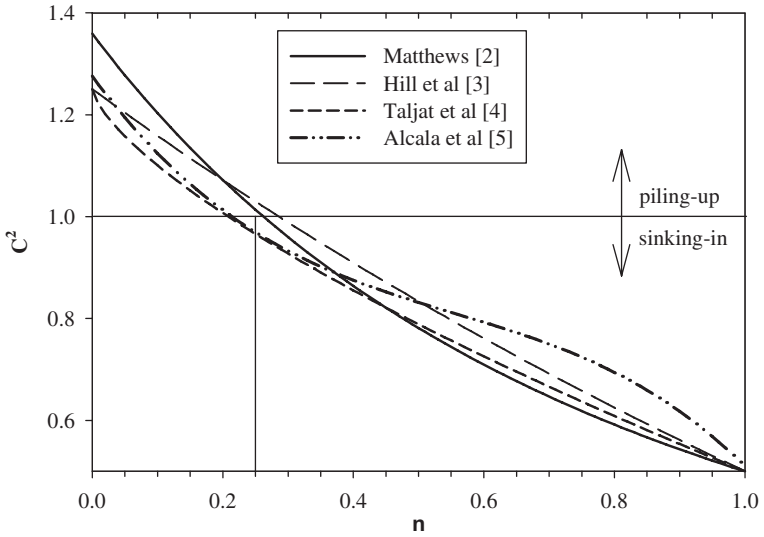

Fig. 2. Evolution of the c^2 parameter obtained with Eqs. (6)–(9) (Matthews, 1980; Taljat et al., 1998; Hill et al., 1989; Alcala et al., 2000).

Indeed, Hill et al. (1989) neglected the occurrence of a linear elastic range and the existence of a well-developed yield stress and Taljat et al. (1998) determined Eq. (8) for an unique value of σ_y/E. On the other hand, it may be that the influence of E and σ_y on the c^2 value was also not observed with experimental results because the range of n values of the studied materials was so large that the yield stress had a weak influence on this parameter. For example, the σ_y/E ratio of the metals tested by Alcala et al. (2000) in order to determine a new c^2 formulation, is in the range from 1/272 to 1/114, whereas the work hardening exponent lies between 0.05 and 0.5. Finally, we must specify that the influence of the friction coefficient between the indenter and indented material was not taken into account in Eqs. (6)–(9)whereas it modifies the surface deformation around the contact area (Mesarovic and Fleck, 1999; Taljat and Pharr, 2004; Mata and Alcala, 2004).

3. Numerical procedure

Numerical simulations were performed with both the rigid spherical indenter of R radius and the rigid parabolic indenter geometry, represented by a curve of equation $z = r^2/R$, where r and z are respectively the radial and the vertical coordinates. These simulations were performed in axisymmetric mode and under frictionless contact conditions ($\alpha = 0$) using the large strain elastic–plastic feature of the Cast3M finite element code. A typical mesh, comprising three-noded isoparametric triangles and four-noded isoparametric rectangles, is shown in Fig. 3.

As shown in this figure, the bottom surface of the specimen has the vertical displacement fixed, whereas a free movement was allowed in the horizontal direction. The parabolic indenter and the spherical indenter are rigid. The shortest distance between nodes along the contact was about $0.002R$ and a maximum of 50 elements became directly in contact with the rigid indenter. The mesh size was chosen so that, in all cases, the contact radius was 20 times smaller than the total length.

The constitutive model of the indented material was taken to follow the well known J_2-associated flow theory with rate-independent deformation and isotropic hardening. Yielding occurs according to the Von Mises criterion and the stress–strain relationship follows the piecewise linear/power-law:

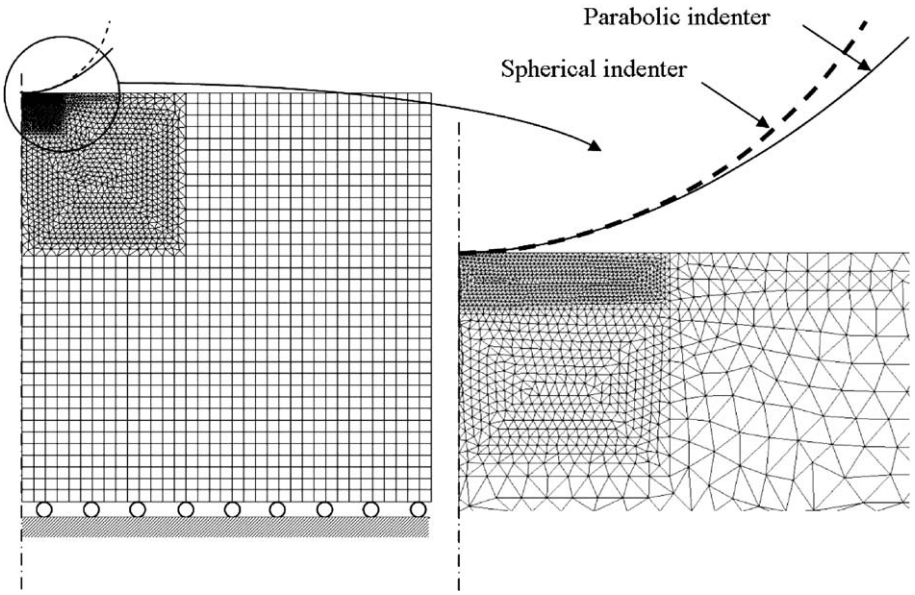

Fig. 3. Typical finite-element mesh, composed of isoparametric axisymmetric elements and rigid parabolic indenter or rigid spherical indenter.

$$\varepsilon = \begin{cases} \sigma/E & \text{if } \sigma < \sigma_y \\ \sigma_y^{(n-1)/n}\sigma^{1/n}/E & \text{otherwise} \end{cases} \tag{10}$$

where ϵ is the total strain, σ is the stress, E is the Young's modulus, σ_y is the yield stress and n is the strain hardening exponent. Finite element simulations were performed for materials exhibiting all possible combinations of $\sigma_y = 50$, 100, 250, 630, 1600, 2500, 4000 and 6300 MPa and $n = 0$, 0.1, 0.2, 0.3 and 0.4. Young's modulus of 210 GPa and Poisson's ratio of 0.3 are used for all simulations. These values were chosen in order to give σ_y/E ratio in the range of 1/4200 to 1/33, which includes most metals.

4. Results of the indentation by a paraboloid of revolution

Examples of h^*–a_p^* ($h^* = h/R$; $a_p^* = a_p/R$, *where* a_p *is the contact radius for parabolic indentation*) relationship obtained for materials with different σ_y/E ratios and n values are presented in Fig. 4. In this figure, the curves can be fitted by two piecewise linear functions in a log-log scale, i.e. piecewise power functions in a linear scale. The first function corresponds to the elastic regime and thus to a small contact radius and the second corresponds to the plastic regime. It can be noted that when yielding occurs, the h^*–a_p^* relationship does not allow an elastic–plastic behavior and a fully plastic behavior to be distinguished, contrary to the applied load–contact radius evolution (Tabor, 1951; Johnson, 1985; Sundararajan and Tirupataiah, 1994; Taljat et al., 1998; Mesarovic and Fleck, 1999; Park and Pharr, 2004).

The h^*–a_p^* evolution is governed in the elastic regime by the following dimensionless Hertz equation:

$$a_p^{*2} = h^* \tag{11}$$

In the plastic regime, the relationship between the true contact radius and penetration depth can be expressed by:

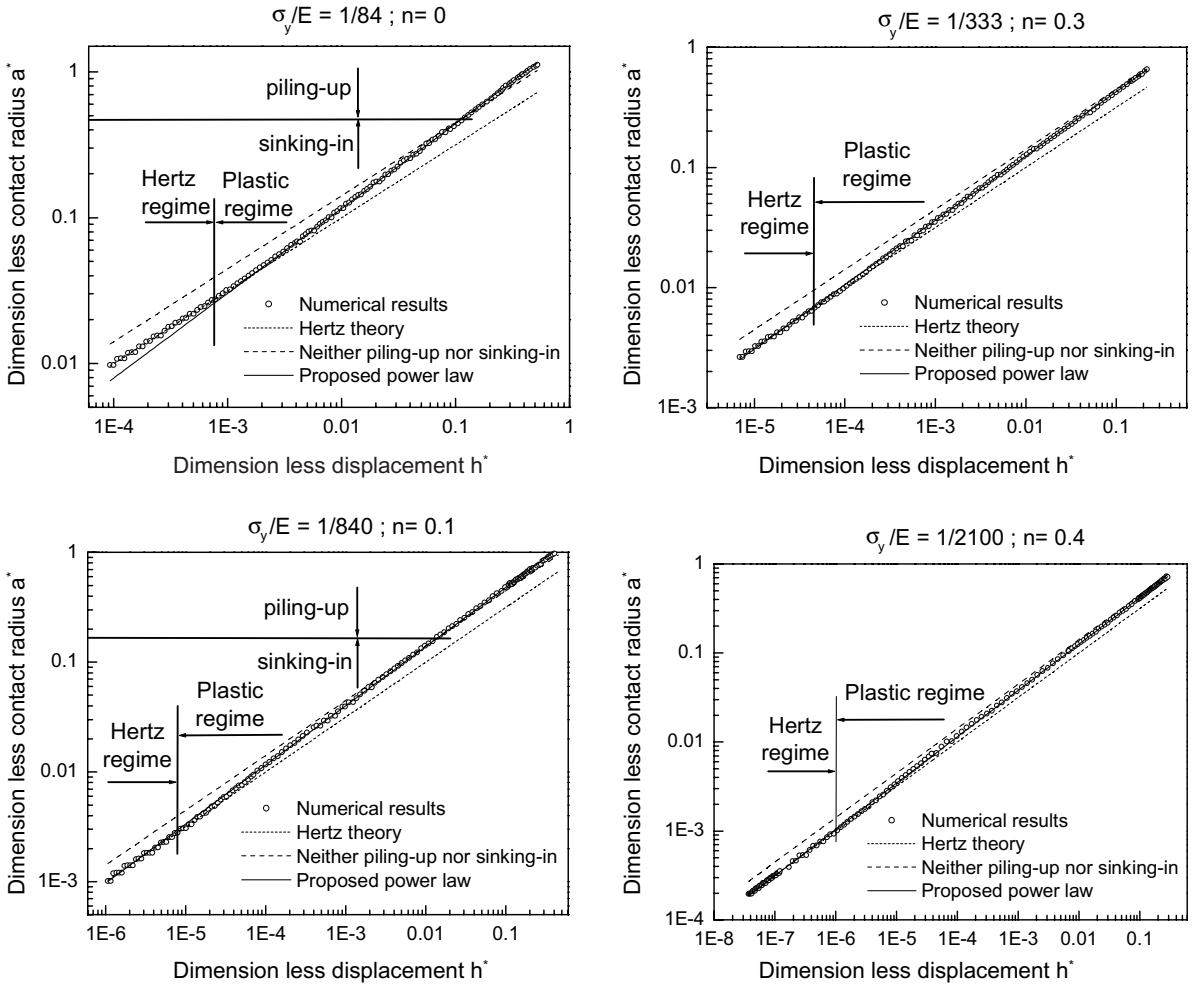

Fig. 4. Examples of contact radius–indentation depth curves for parabolic indentation.

$$a_{\mathrm{p}}^{*N} = 2Mh^{*} \tag{12}$$

where M and N are constant for a given indented material.

The analysis of the 25 h^{*}–a_{p}^{*} numerical curves allows the M and N coefficients to be expressed by the functions:

$$M = \frac{\left(1.45 + 28.55n + 1745\sigma_{\mathrm{y}}^{*}\right)\left(1 - 0.5n + 20\sigma_{\mathrm{y}}^{*}\right)}{\left(1 + 21.4n + 1020\sigma_{\mathrm{y}}^{*}\right)\left(1 + 0.4n + 60\sigma_{\mathrm{y}}^{*}\right)}$$
$$N = \frac{\left(1.9 + 12.5n + 570\sigma_{\mathrm{y}}^{*}\right)(1 + 0.1n)}{\left(1 + 6.8n + 340\sigma_{\mathrm{y}}^{*}\right)} \tag{13}$$

where σ_{y}^{*} is equal to σ_{y}/E.

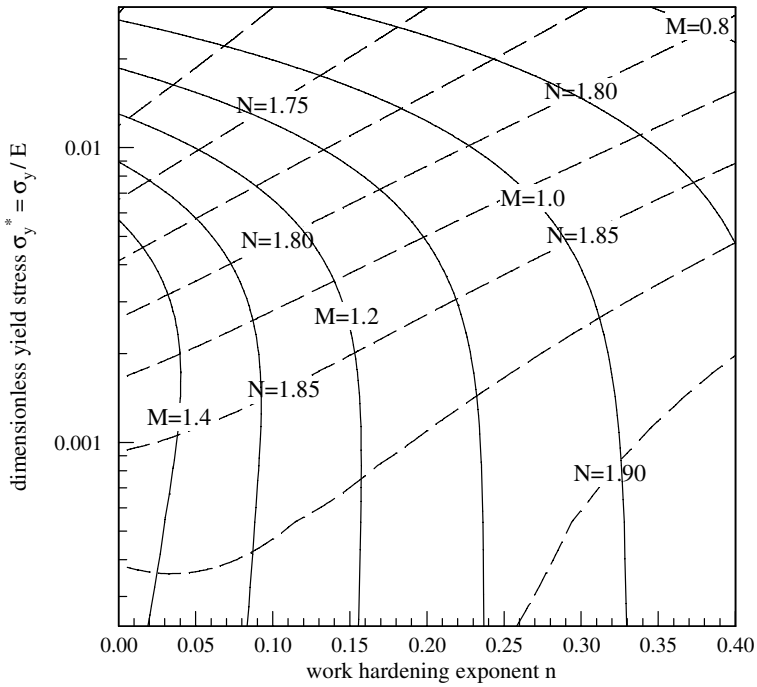

Fig. 5. N and M coefficients versus σ_y^* and n. The solid lines correspond to M coefficients and the dash lines correspond to N.

We can notice in Eq. (13) that M and N are dependent on the σ_y/E ratio and the work hardening exponent n. Fig. 5 shows the M and N evolution according to σ_y/E and n.

Results given in this figure indicate that N values are always smaller than 2. Thus, the slope $(1/N)$ of the h^*–a_p^* in log–log scale is always higher than 0.5, which is the value of the slope of the "neither piling-up nor sinking-in" curve (Fig. 4). Consequently, piling-up occurs for any material indented by a paraboloïd of revolution starting from the following critical contact radius:

$$a^*_{pcrit} = M^{1/(N-2)} \tag{14}$$

This is a noticeable difference compared to the spherical indentation and the conical indentation, for which, piling-up occurs or not according to the material properties because of the indenter geometry (Matthews, 1980; Taljat et al., 1998; Beghini et al., 2000; Alcala et al., 2000; Kucharski and Mröz, 2001; Mata et al., 2002).

The smaller the strain hardening exponent, the smaller the value of a^*_{pcrit} (Fig. 6). According to previous results (Matthews, 1980; Hill et al., 1989; Taljat et al., 1998; Beghini et al., 2000; Alcala et al., 2000; Kucharski and Mröz, 2001; Mata et al., 2002; Taljat and Pharr, 2004), this shows that the smaller the strain hardening exponent is, the earlier the pile up arises. However, contrary to those of different researchers (Matthews, 1980; Hill et al., 1989; Taljat et al., 1998; Alcala et al., 2000; Kucharski and Mröz, 2001), the present results show that the h^*–a_p^* relationship is dependent on the material yield stress. Small values of N and high values of a^*_{pcrit} are obtained for high σ_y/E ratio. The influence of material yield stress on the h^*–a^* evolution has been recently observed for conical indentation (Mata et al., 2002) and spherical indentation (Beghini et al., 2000). For Mata et al. (2002), this influence exists when a linear elastic behavior is not neglected and when a well-developed yield stress exist, which is the case for the present study.

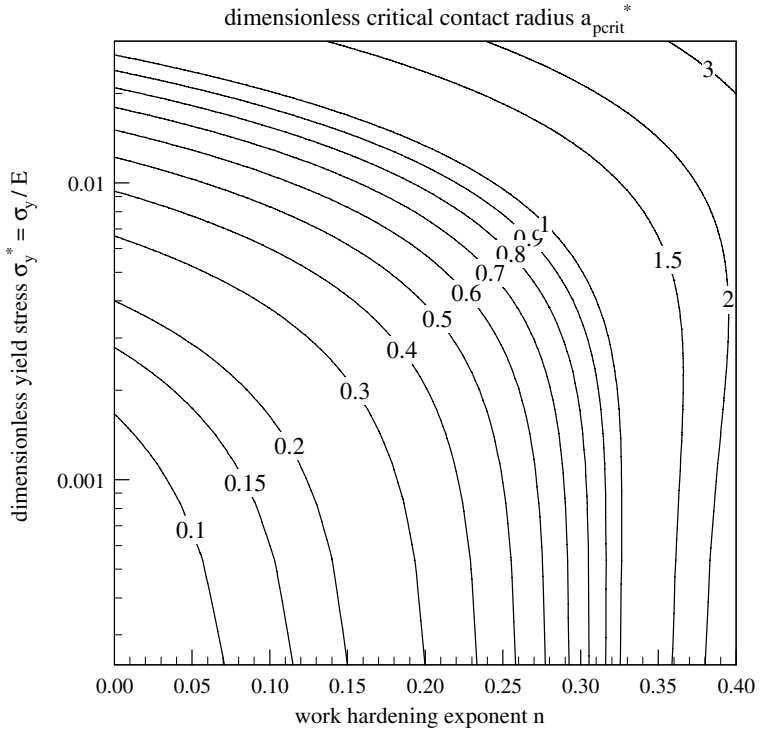

Fig. 6. Dimensionless critical contact radius, for which piling-up appears in the case of parabolic indentation, in function of σ_y^* and n.

5. Adaptation of the model for spherical indenter

The study of parabolic indentation was useful in order to distinguish the influence of the material and the geometrical properties on the relationship between the contact radius and the penetration depth. However, the study of spherical indentation is necessary because the ball indenter is a precision instrument which is easy to make, yet robust, inexpensive and thus often used for experimental tests.

Because the spherical indenter is very similar to the parabolic indenter for small contact radius, the evolution of the dimensionless contact radius between the sphere and the indented material, a_s^*, in function of the penetration depth, can be fitted by a power law in the beginning of the plastic regime. However, Fig. 7 shows that this is not the case when the contact radius is large. Indeed, the use of the power function given in Eqs. (12) and (13), enables the numerical data to be fitted correctly until a critical value of dimensionless contact radius, about equal to 0.3, is reached. This value corresponds approximately to the higher limit for which the spherical indenter can be represented by a parabolic function (difference of 1% between a_s^* and a_p^*). Fig. 7 shows that a_s^* can be geometrically determined starting from the a_p^* value by using the following equation:

$$a_s^* = a_p^* \sqrt{1 - a_p^{*2}/4} \tag{15}$$

This equation was established using the assumption that the penetration depth is hardly influenced by the difference in geometry between the spherical and the parabolic indenters. Compared with the previous formulations (Matthews, 1980; Hill et al., 1989; Taljat et al., 1998; Alcala et al., 2000; Kucharski and Mröz,

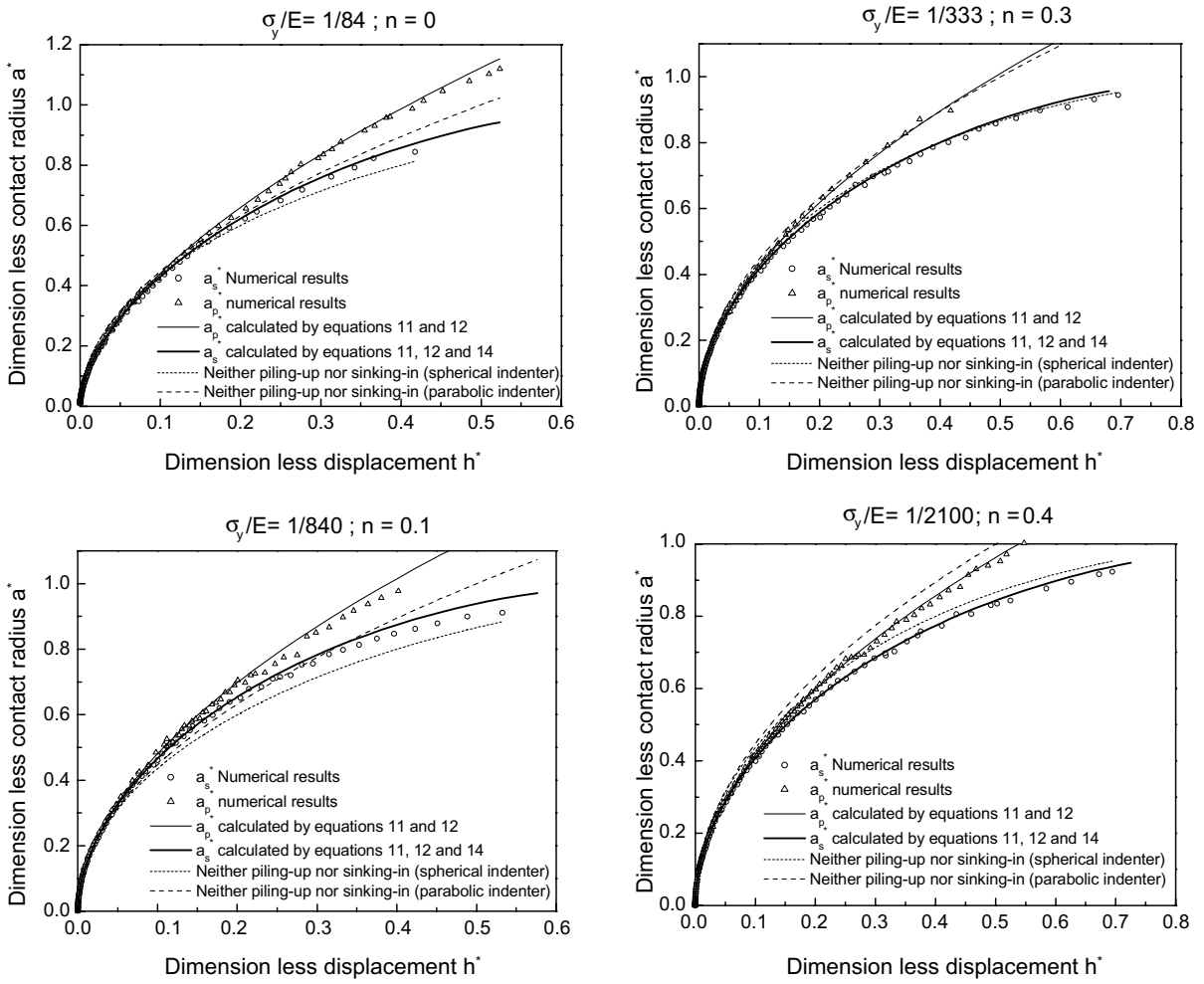

Fig. 7. Examples of dimensionless contact radius–indentation depth curves for parabolic and spherical indenters.

2001), the interesting aspect of the proposed Eqs. (12), (13) and (15) is that they lead to a relationship between the true contact radius and the penetration depth valid, for spherical indenters, in the elastic–plastic and fully plastic regimes (Fig. 7). This relationship is true until a large dimensionless contact radius is reached (about 0.8 corresponding to a value of h^* of about 0.4).

6. Analytical determination of the h_c/h ratio

6.1. Parabolic indentation

Piling-up occurs when the (h_c/h) ratio is higher than 1 whereas sinking-in occurs when this ratio is smaller than 1 (Fig. 1). This criterion is valid for parabolic or spherical indentation.

For a parabolic indentation, the results presented in Section 4 showed that the height/depth of the pile-up/sink-in from the original surface depends on the contact radius. Starting from Eq. (12) and the equation of the parabolic curve, the (h_c/h) ratio can be expressed for material plastically deformed by the parabolic indenter as follows:

$$\frac{h_c}{h} = M a_p^{*2-N} = M^{2/N}(2h^*)^{(2-N)/N} \tag{16}$$

Examples given in Fig. 8 show that there is a strong similarity between the h^*–(h_c/h) relationship calculated by using Eq. (16) and that obtained by finite element simulations when plasticity occurs. The results confirm that the higher the contact radius, the more the piling-up is predominant, in the case of parabolic indentation.

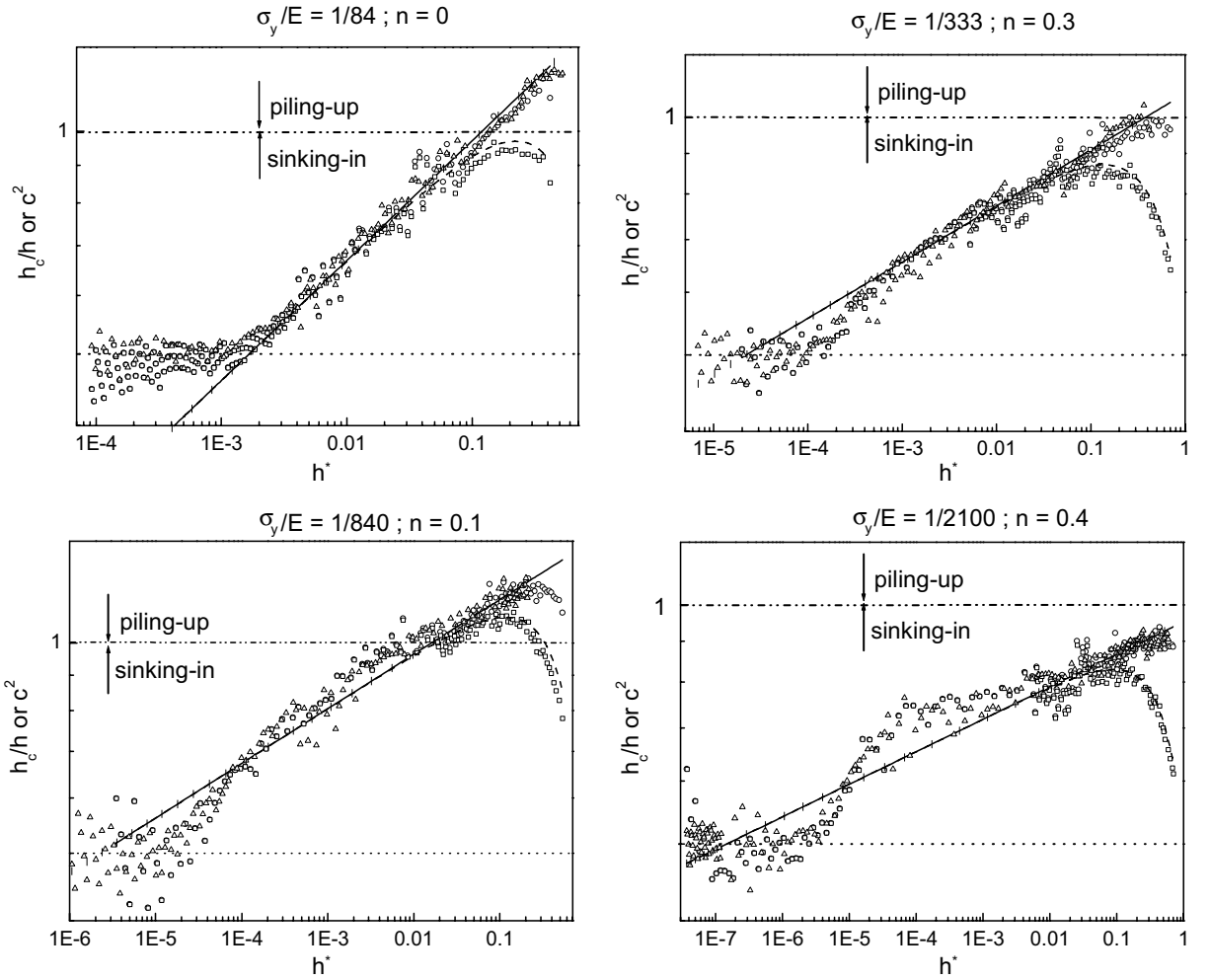

Fig. 8. Comparison between true contact depth–penetration depth ratio and c^2 parameter. Parabolic indentation: (△) numerical results; (▪▪▪) calculated by Eq. (16); (▪▪▪) Hertz. Spherical indentation: (○) numerical results; (—) calculated by Eq. (19); (□) c^2, numerical results ; -- c^2, calculated by Eq. (17).

6.2. Spherical indentation: use of the c^2 parameter

For spherical indentation, Hill et al. (1989) proposed to replace the (h_c/h) ratio by the c^2 parameter defined in Eq. (1). By using Eqs. (1), (12) and (15), the c^2 parameter can be written for material plastically deformed by the spherical indenter, as follows:

$$c^2 = \frac{a_s^{*2}}{2h^*} = M^{2/N}(2h^*)^{(2-N)/N}\left(1 - \frac{(2Mh^*)^{2/N}}{4}\right) \tag{17}$$

This equation shows that c^2 is dependent on the dimensionless penetration depth h^* or on the dimensionless contact radius a_s^*. Fig. 8 shows that when a_s^* or h^* increases, the c^2 parameter is constant in the elastic regime, then increases in a first stage of the plastic regime and decreases at the end of this regime.

Our results are in agreement with the numerical results obtained by Mesarovic and Fleck (1999) for the high values of σ_y/E ratio. It can be seen in Fig. 8 that the decrease of c^2 occurs for values h/R ratio higher than approximately 0.15. This value corresponds to a value of dimensionless contact radius of approximately 0.5. However, for this range of h/R or a/R values, the definition of c^2 given by Hill et al. (1989) is not correct because the spherical indenter can't be considered as similar to the parabolic indenter, i.e. $h/(2R)$ can not be considered as very small compared to 1.

If the values of the c^2 parameter are compared to those of the h_c/h ratio, it can be seen that c^2 corresponds to h_c/h for small deformations. However, c^2 is much smaller than h_c/h when the dimensionless penetration depth is higher than 0.1. Above this value, corresponding to a value of a^* of about 0.4, the use of the c^2 parameter has as a consequence a noticeable underestimation of the contact depth and thus of the contact radius. For example, in the case of a spherical indentation of a material of $\sigma_y/E = 1/84$ and $n = 0$, the value of the h_c/h ratio indicates that piling-up occurs starting from a critical value of h^* of approximately 0.12, whereas the c^2 parameter indicates sinking-in for all contact radius values.

6.3. Spherical indentation: use of the $c'^2 = (h_c/h)$ parameter

In order to avoid errors in the case of large values of h^*, the true relationship between a_s^* and the dimensionless penetration depth must be written as follows:

$$a_s^{*2} = c'^2(2h^* - c'^2h^{*2}) \tag{18}$$

In this equation, we introduce a parameter c'^2 equal to the h_c/h ratio. This parameter is equal to 1 when neither piling-up nor sinking-in occurs but is different to the c^2 parameter defined by Eqs. (6)–(9) in the case of plastically indented material.

The c'^2 parameter, equal to h_c/h can be written as follows:

$$c'^2 = \frac{h_c}{h} = M\left[2\left(1 - \sqrt{1 - a_s^{*2}}\right)\right]^{(2-N)/2} = M^{2/N}(2h^*)^{(2-N)/N} \tag{19}$$

This relationship was established by using Eqs. (12), (15) and (18) and thus is valid up to a dimensionless contact radius of about 0.8. The h^*–c'^2 relationship defined by Eq. (19) in the case of spherical indentation is equivalent to the h^*–(h_c/h) relationship defined for the parabolic indentation (Eq. (16)). The numerical results given in Fig. 8 confirms that the difference of shape between the spherical and parabolic indenters has little influence on the h^*–(h_c/h) relationship throughout the domain where Eqs. (15) and (19) are valid. Moreover, if we consider h^* values lower than 0.3, the numerical results show that, as for parabolic indentation, the h_c/h is constant when a material is elastically deformed by a spherical indenter but is never constant when plasticity occurs. The results obtained by Eq. (19), proposed in order to describe h_c/h, are in good agreement with the results obtained by Taljat and Pharr (2004) for a material of $\sigma_y/E = 1/200$ and $n = 0$ when sinking-in occurs (Fig. 9). However, there is a consistent gap when piling-up predominates. The reason

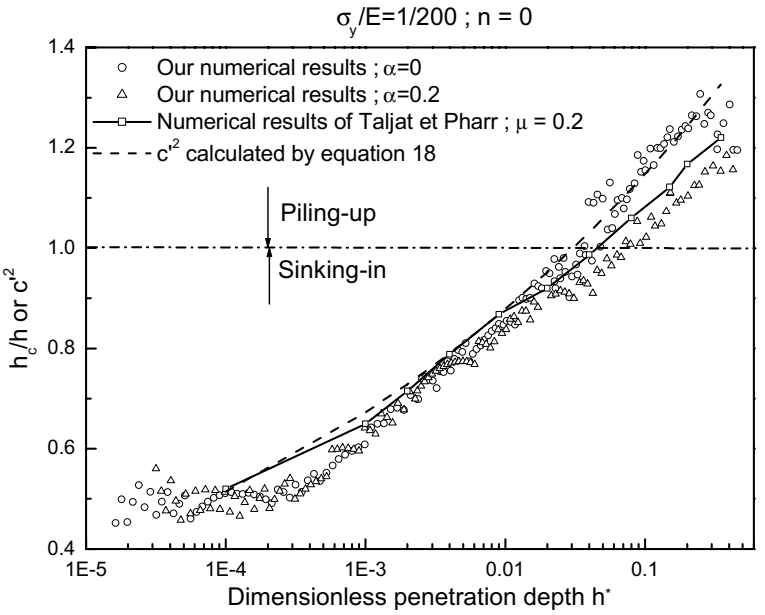

Fig. 9. Comparison between the h_c/h values calculated by Eq. (19) and those numerically obtained by Taljat and Pharr (2004).

for this gap is that the friction coefficient between the indenter and the material is higher for the Taljat and Pharr's simulation ($\alpha = 0.2$) compared to the simulations used in order to determine the Eq. (19) ($\alpha = 0$). Indeed, according to the results of Mata and Alcala (2004) and Taljat and Pharr (2004), a numerical simulation performed with a friction coefficient equal to 0.2 shows that an increase in friction coefficient reduce the h_c/h ratio in the case of pile-up but has little influence in the case of sink-in.

Lastly, for the a^* values higher than 0.8, the numerical values of $c'^2(=h_c/h)$ are constant or decrease because of the high value of the angle, β ; between the tangent line to the contact at its periphery and the undeformed surface (Fig. 1). Indeed, angle β, close to 90°, facilitates the rupture of contact between the indenter and the indented material at the periphery of the contact.

6.4. Discussion about the previous analytical formulation of c^2

The preceding results showed that the value of the c^2 parameter increases with the penetration depth when the definition of this parameter is valid. In consequence, the previous Eqs. (6)–(9) (Matthews, 1980; Hill et al., 1989; Taljat et al., 1998; Alcala et al., 2000) established in order to determine the h_c/h and dependent only on the strain hardening exponent are valid only for a given penetration depth. Fig. 10a confirms this observation. Indeed, it can be seen in this figure that the values obtained by the Matthews's formulation (Eq. (6)) are close to those determined by c'^2 in the case of an indented material of σ_y/E ratio equal to 1/2100 and for a dimensionless contact radius in the range from 0.5 to 0.6. The reason for this closeness is due to the fact that the Matthews's formulation was determined starting from a fit to the Norbury and Samuel h_c/h versus n experimental results obtained at a depth for which a/R was mostly between 0.4 and 0.8. The other curves calculated by Eqs. (7)–(9) in the case of a same indented material are only approximate to our results obtained when a_s^* is in the range from 0.3 to 0.4, which is coherent with the assumptions of the different authors (Hill et al., 1989; Taljat et al., 1998; Alcala et al., 2000). The condition on the penetration depth is not the only one in order to obtain correct results with these c^2 analytical formulations because when a_s^* is equal to 0.4 and σ_y/E is smaller than 1/333 a strong difference

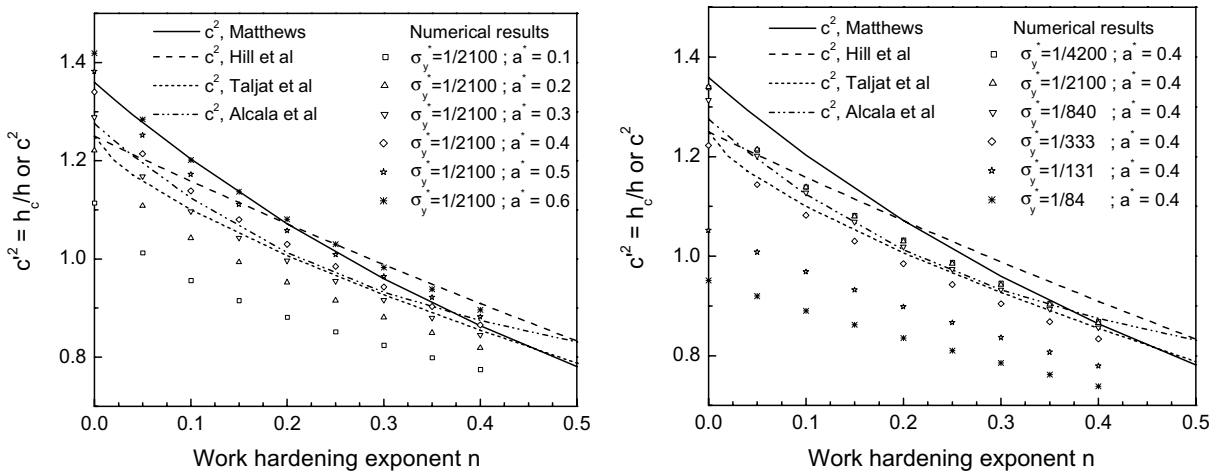

Fig. 10. Comparison between the c^2 parameter calculated by using Eqs. (6)–(9) and the $c'^2(=h_c/h)$ parameter for different contact radius, work hardening exponents and σ_y/E ratios.

exists between c^2 calculated by using Eqs. (6)–(9) and $c'^2 = h_c/h$ (Fig. 10b). This figure shows that the higher the σ_y/E ratio, the smaller the h_c/h, which is in good agreement with recent results obtained for spherical indentation (Beghini et al., 2000; Taljat and Pharr, 2004) and conical indentation (Mata et al., 2002). Thus, for large σ_y/E ratios, the use of Eqs. (6)–(9) has, as a consequence, a large overestimation of the h_c/h ratio.

In conclusion, because of the assumptions of the different authors (Matthews, 1980; Hill et al., 1989; Taljat et al., 1998; Alcala et al., 2000), the analytical formulations (6)–(9) established in order to determine the contact radius starting from the knowledge of the penetration depth, lead to acceptable results only for a given penetration depth and when σ_y/E is smaller than about 1/333.

7. Discussion about the development of the pile-up

For the studied range of materials, we determine the relationship between the mechanical properties of the material, i.e. the σ_y/E ratio and n, and the dimensionless contact radius, a^*_{scrit}, starting from which the pile-up appears. By using Eqs. (14) and (15), the critical a^*_{scrit} can be expressed as follows:

$$a^*_{scrit} = a^*_{pcrit}\sqrt{1-\frac{a^{*2}_{pcrit}}{4}} = M^{1/(N-2)}\sqrt{1-\frac{M^{2/(N-2)}}{4}} \tag{20}$$

As for Eqs. (15), this formulation is correct up to an a^*_s value about equal to 0.8.

Fig. 11 shows the evolution of the critical a^*_{scrit} values according to the σ_y/E ratio and the strain hardening exponent n. In the case of material with small yield stress, it can be seen in this figure that piling-up appears for a value of work hardening exponent of approximately 0.22 when the critical contact radius is in the range of 0.3–0.4. This work hardening exponent value is similar to that calculated by Eqs. (6)–(9) proposed by different researchers (Matthews, 1980; Hill et al., 1989; Taljat et al., 1998; Alcala et al., 2000).

We demonstrated, in the case of parabolic indentation, that the higher the σ_y/E ratio, the later the pile up arises. For spherical indentation, the same behaviour is observed but because of the indenter shape, piling-up may not appear, especially for high values of n and high values of σ_y/E ratio. On the basis of numerical results, we can consider that no piling-up occurs for spherical indentation when the M parameter defined in

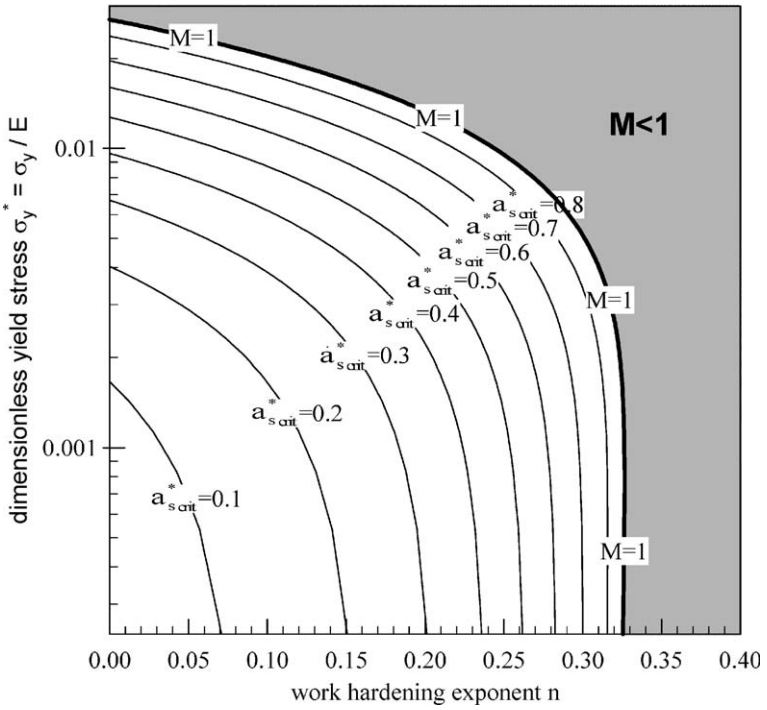

Fig. 11. Critical contact radius, for which piling-up appears in the case of spherical indentation, versus σ_y/E ratio and strain hardening exponent n. In the area where M is smaller than 1, piling-up never appears.

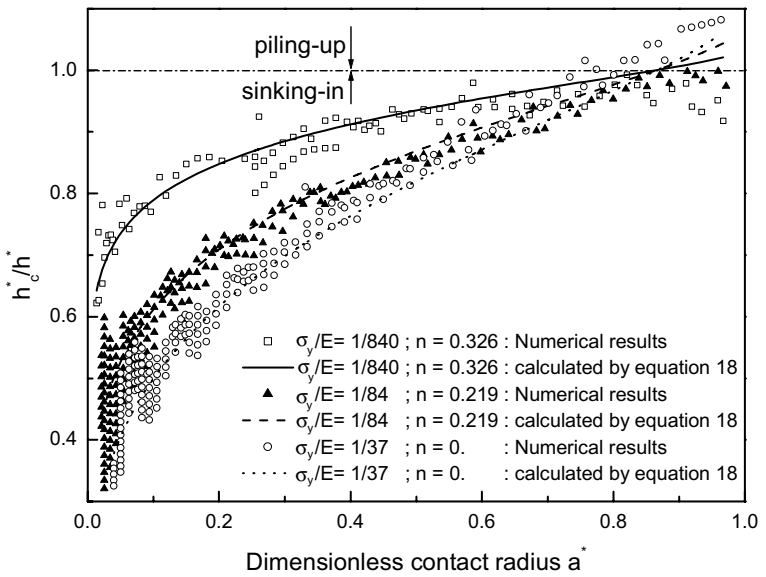

Fig. 12. h_c/h ratio as a function of the dimensionless contact radius for three materials of $M = 1$.

Eq. (13) is smaller than 1 (Fig. 11). Indeed, the a^*–(h_c/h) curves obtained numerically for three different indented materials of $M = 1$ show that the values of the critical contact radius a_s^*, for which the pile-up appears, is equal to $\sqrt{3/2} \approx 0.87$ (Fig. 12). Fig. 12 shows that the numerical results obtained for these three materials are close to those calculated by Eq. (19) up to a dimensionless contact radius of 0.8 (limit of the validity domain of Eq. (19)). Beyond this limit, three types of behaviours are observed depending on the material. For the material of $\sigma_y/E = 1/84$ and $n = 0.219$, The h_c/h ratio increases slightly up to a value of h_c/h of approximately 1. For the material of $\sigma_y/E = 1/840$ and $n = 0.326$, the h_c/h ratio does not increase significantly and the value of this ratio is slightly lower than 1. For the last material characterized by a σ_y/E ratio and a work hardening exponent respectively equal to 1/33 and 0, the h_c/h ratio increases and the value of this ratio exceeds 1. In conclusion, the criterion $M < 1$ is not perfect but is valid in order to determine when the pile-up does not appear for most of the spherically indented materials.

8. Conclusion

New formulations are proposed in order to determine the indentation depth–contact radius relationship in the case of parabolic and spherical indentations. In a first step, it is shown, for parabolic indentation, that the contact radius evolution, a_p, in function of the penetration depth, h, is governed by two piecewise power functions. The first function corresponds to the elastic regime and the second corresponds to the plastic regime. A new power law is proposed in order to determine the h–a relationship in the plastic regime for a rigid parabolic indenter and an indented material of Poisson's ratio of 0.3. The parameters of the proposed power law depend on the yield stress and the strain hardening coefficient of the indented material. The values of these parameters show that piling-up occurs for any material indented by a paraboloïd of revolution starting from a critical contact radius. This is a noticeable difference compared to spherical indentation and conical indentation, for which, piling-up or sinking-in occurs or not in the fully plastic regime, depending on the material. It can be also noticed that the smaller the strain hardening coefficient, the earlier the pile up arises. Similarly, the smaller the σ_y/E ratios, the earlier the pile up arises. The same conclusion is drawn for small n. Then, a geometrical adaptation was performed in order to determine the h–a_s evolution for a rigid spherical indenter starting from the power law proposed for the parabolic indentation. From our results, we show that the previous equations proposed in order to determine the penetration depth–contact radius relationship are only valid for a given penetration depth and for materials of small yield stress. The formulation proposed in the present study for spherical indentation has the advantage of being correct in the plastic regime up to a dimensionless contact radius of about 0.8 and for materials of σ_y/E ratios in the range of 1/4200 to 1/33. Lastly, a simple criterion, depending on the material mechanical properties, is proposed in order to know when piling-up appears for the spherical indentation.

References

Alcala, J., Barone, A.C., Anglada, M., 2000. The influence of plastic hardening on surface deformation modes around Vickers and spherical indents. Acta Metallurgica 48, 3451–3464.

Beghini, M., Bertini, L., Fontanari, V., 2000. Evaluation of the flow curve of metallic materials by means of spherical indentation. Computational Methods in Contact Mechanics V, 241–252.

Bolshakov, A., Pharr, G.M., 1998. Influences of pileup on the measurement of mechanical properties by load and depth sensing indentation techniques. Journal of Materials Research 13 (4), 1049–1058.

Eskner, M., Sandström, R., 2004. Measurement of the elastic modulus of a plasma- sprayed thermal barrier coating using spherical indentation. Surface and Coatings Technology 187 (1), 113–121.

Hill, R., Stôrakers, B., Zdunek, A.B., 1989. A theoretical study of the Brinell hardness test. Proceedings of the Royal Society of London A 423, 301–330.

Johnson, K.L., 1985. Contacts Mechanics. Cambridge University Press, Cambridge, UK.
Kucharski, S., Mröz, Z., 2001. Identification of plastic hardening parameters of metals from spherical indentation tests. Materials Science and Engineering A 318, 65–76.
Mata, M., Alcala, J., 2004. The role of friction on sharp indentation. Journal of the Mechanics and Physics of Solids 52 (1), 145–165.
Mata, M., Anglada, M., Alcala, J., 2002. Contact deformation regimes around sharp indentations and the concept of the characteristic strain. Journal of Materials Research 17 (5), 964–976.
Matthews, J.R., 1980. Indentation hardness and hot pressing. Acta Metallurgica 28, 311–318.
Mesarovic, D.J., Fleck, N.A., 1999. Spherical indentation of elastic–plastic solids. Proceedings of the Royal Society of London A 455, 2707–2728.
Meyer, E., 1908. Untersuchen über Härteprüfung und Härte. Zeitschrift des Vereins Deutschen Ingenieure 52, 645–654.
Norbury, A., Samuel, T., 1928. The recovery and sinking-in or piling-up of material in the Brinell test, and the effect of these factors on the correlation of the Brinell with certain other hardness tests. Journal of the Iron Steel Institute 117, 673–687.
Oliver, W.C., Pharr, G.M., 1992. An Improved technique for determining hardness and élastique modulus using load and displacement sensing indentation experiments. Journal of Materials Research 7 (6), 1564–1583.
O-Neill, H., 1944. The significance of tensile and other mechanical test properties of metals. Proceedings of the Institute of Mechanical Engineers 151, 116–130.
Park, Y.J., Pharr, G.M., 2004. Nanoindentation with spherical indenters: finite element studies of deformation in the elastic–plastic transition regime. Thin Solid Films 447–448 (30), 246–250.
Sneddon, I.N., 1965. The relation between load and penetration in the axisymmetric Boussinesq problem for a punch of arbitrary profile. International Journal of Engineering Science 3, 47–57.
Sundararajan, G., Tirupataiah, Y., 1994. The hardness-flow stress correlation in metallic materials. Bulletin of Material Science 17 (6), 747–770.
Tabor, D., 1951. The Hardness of Metals. Clarendon Press, Oxford, UK.
Taljat, B., Pharr, G.M., 2004. Development of pile-up during spherical indentation of elastic–plastic solids. International Journal of Solids and Structures 41 (14), 3891–3904.
Taljat, B., Zacharias, T., Kosel, T., 1998. New analytical procedure to determine stress–strain curve from spherical indentation data. International Journal of Solids and Structures 35 (33), 4411–4426.